Transportation Engineering 6 (2021) 100098

Contents lists available at ScienceDirect

Transportation Engineering

journal homepage: www.sciencedirect.com/journal/transportation-engineering

Development of an in-vehicle power line communication network with *in-situ* instrumented smart cells

Timothy A. Vincent *, Begum Gulsoy, Jonathan E.H. Sansom, James Marco

Cell Instrumentation Team, WMG, University of Warwick, UK

ARTICLE INFO

Keywords:
Cell communication network
Cell instrumentation
In-situ cell temperature sensing
Real-time dynamic measurements
Vehicular power line communication

ABSTRACT

Instrumented cells, equipped with miniature sensors, are proposed to aid the next stage of electrification in the automotive and aerospace industries. To optimize the energy density available within a lithium ion (li-ion) pack we demonstrate how a power line communication (PLC) network can be formed at an individual cell level. This reduces the need for complex communication cables within a vehicle wiring loom.

Here we show a unique prototype smart cell (instrumented cell equipped with interface circuitry and processing capability) can be connected via a PLC network, to enable monitoring of vital parameters (temperature, voltage, current), regardless of cell state of charge (2.5 V to 4.2 V DC operating voltage). In this proof-of-concept study, we show the reliable system (0 errors detected over ~24 hr experiment, acquired data (logged at 10 Hz) from cells (in a parallel configuration), and comparative data for cell internal and external temperature was recorded. During a prolonged discharge (1C, 5A discharge) a peak core temperature >3 °C hotter than surface temperature was observed, highlighting the need to understand cell operation in cooling system design.

1. Introduction

Power Line Communication (PLC) enables data networks to be created in environments where only power wiring is available between nodes, perhaps when either cost or physical space would otherwise prohibit communication cabling. Considering battery energy applications, there have been previous reports of PLC connecting high voltage networks, such as solar panel farms and remote energy plants, to base stations [1, 2]. In terms of in-vehicle applications, PLC has been proposed to enable peripherals to be integrated around a vehicle (e.g. electric mirror adjustment [3] or reversing cameras [4]), reducing the cost, weight and complexity of the wiring loom.

We have previously reported successfully integrating PLC within a small (4 series, 2 parallel - 4S2P - configuration of eight 21,700 cells) module, allowing communication between interface nodes around the module to a central logging node (2 slave modems, 1 master) [5]. In this work we move towards our goal of smart cells replacing their current passive counterparts. Previously the physical size of the modem and interface circuitry prevented installation on an individual cell basis.

In this work we demonstrate a novel revised miniature modem and interface circuitry system (20 mm diameter PCB) which can be powered from an individual cell across its full state-of-charge voltage range (2.5 V to 4.2 V DC). To the authors' knowledge, there are no previous reports in the literature combing instrumented cells with PLC circuity. Hu et al. [4, 6], demonstrated an in-vehicle PLC system powered by the 12 V DC supply inside a car. This system removed the traditional dedicated communication wiring for a reversing camera, although avoided the complexity of testing PLC across a variable DC voltage powerline and did not discuss the bandwidth restrictions if multiple nodes were added to the network. We have developed and tested a system capable of transmitting acquired sensor data via a power line, of variable DC voltage, with processing and transmission performed on an individual cell level.

The PSOC 5lp (Cypress Semiconductor) was tested by Saleem [7], towards use in a vehicular application. The study did not comprehensively test the modems at different powerline voltages, nor when current was drawn from the supply. Jousse et al. [10] replaced wiring between two CAN (Controller Area Network) nodes with a PLC link. This demonstrates the PLC connection had sufficient bandwidth to meet the requirements of a basic CAN system, although fails to capture the ambition to integrate PLC within a vehicle from first principles (i.e. data is sent directly via PLC, without conversion from CAN to PLC).

In a study by Landinger et al. [8], PLC functionality was demonstrated with six cylindrical cells connected serially, although, again, the

* Corresponding author.
E-mail address: T.A.Vincent@warwick.ac.uk (T.A. Vincent).

https://doi.org/10.1016/j.treng.2021.100098
Received 10 September 2021; Received in revised form 19 November 2021; Accepted 20 November 2021
Available online 23 November 2021

system was not tested when the cells were cycled. Talie et al. [9] demonstrated data integrity was maintained when transmitting via PLC with a small module of cylindrical cells. However, the system was limited to testing only simulated data, generated on a microprocessor (18 bits in length). Furthermore, the reported data only demonstrated functionality over a period of a few seconds. In our work we test the PLC network with transient sensor data (current, voltage and temperature monitoring), which demonstrates the system is suitable and capable of processing and transmitting realistic data loads in real time. In this article, we present the results and findings from our proof-of-concept study, including 2 instrumented 21,700 format cylindrical cells, transmitting data via the low-voltage DC powerline.

Uniquely our study demonstrates the reliability of the cell powered PLC network over a period of >24 hrs, including the transmission and receiving of thousands of messages per hour. The cells are internally instrumented with flexible thermistor circuitry, enabling core temperature to be monitored during our cycling experiments. Data from two cells (21,700, 2P configuration) are collected via PLC at a rate of 10 Hz per cell.

We have structured this article as follows: Our motivation behind developing instrumented cells with PLC; the design of our experiments and setup; initial results from instrumented cells demonstrating low-voltage PLC and conclusions of our study and ongoing work.

2. Motivation

Inside a battery pack, monitoring the internal core temperature of a cell is important during both the conceptualisation and development of the pack, and during its final application. Internal measurements have been noted to offer reliable data for li-ion cell modelling as well as a greater understanding into the demands from an individual cell (opposed to either external or theoretically derived measurements) [11]. Current automotive packs lack internal sensing (relying solely on <20 surface data points, for packs containing many hundreds of cells [12]).

Prediction of a thermal event (i.e. extreme case, thermal runaway), monitoring of internal temperature is vital to enable early detection (and therefore prevention), where fluctuations in internal temperature that do not register externally, can help identify hot-spots within the cell [13]. This is of particular importance in the aerospace industry, and in other such applications with harsh environmental conditions (sub-freezing etc. [14]), where the operation of cells is less well studied and safety and reliability are of paramount importance.

Manufacturers must currently make a trade-off between instrumentation spatial resolution, pack monetary cost, energy density (pack energy density decreases to 170 Wh/kg with li-ion cells, compared to 250 Wh/kg for an individual cell [15]) and interface hardware complexity [13]. Communication cabling must be resilient to vibration (needed to ensure reliability [16]). Poor design of cooling systems can exacerbate non-uniform heating (and therefore ageing) [17]. During pack operation, cell failure is difficult to predict; perhaps manufacturing flaws manifesting over time, internal short circuits are noted as a common failure mode) [18]. Automotive packs often contain thermocouple sensors [19], although these are difficult to connect sequentially (each requires cold junction [20]).

Next generation sensors, such as optic fibres, have been suggested for pack instrumentation (distributed sensing) [21], although their high cost is prohibitive for small modules. In this work thermistor sensors were selected, offering a distributed sensing (flexible array designed with 10 mm spatial resolution), high accuracy (0.1 °C [22]) and low cost (<$0.01 each).

PLC offers a solution to enable smart cells to be integrated into a pack without the burden of additional cabling (weight, complexity). Furthermore, it removes the electronic complexity that occurs when performing measurements without a common ground (each cell negative terminal could be considered a separate ground). It is proposed each smart cell contains self-powered sensors and acquisition hardware which would prevent overloading the BMS (Battery Management System) with initial signal processing duties of hundreds of sensors. Integration with a CAN bus for example, has been trialled in our other work, but requires ground isolation between each cell.

In this work we test low-bandwidth PLC (5 MHz, up to 500 kbit/s) in a bi-directional network (enabling communication from master to slave cells for reporting data and vice versa to permit control of the cells, e.g. vary measurement parameters). We test using a buck-boost voltage regulator to enable the circuitry to operate across the full state-of-charge voltage range of the cell (PLC tested between 2.5 to 4.2 V DC).

3. Methodology

The communication system comprises 3 blocks, shown in Fig. 1. PLC modems are contained on each cell and at the receiver (BMS, in this case represented by a data logging computer). In total, 3 PLC modems are required in this experiment; 2 are configured as slaves (predominately transmitting data) and 1 is the master (predominately receiving the sensor data and sending commands). To address each node, a unique serial number is assigned via firmware. The PLC occurs over the brass bus bars, which also form the electrical power connection between the cells and the cycling equipment.

The PLC modem THVD8000DDFR from Texas Instruments (TI, USA) was selected, offering small size (2.9 × 1.6 mm, small outline transistor, SOT-23 (8) package), low cost (<$3 even at relatively low volume), low operating voltage (3.0 to 5.5 V DC) and extended temperature range (−40 to 125 °C) [23]. The modem dissipates up to 100 mW during transmission. During typical operation, when in receive mode, the PCB consumes a total of less than 30 mW. It is proposed this consumption could be reduced, by removal of prototyping components (such as the LED and USB data interface), as well as optimising the ADC sampling rate and resolution. The 5 MHz operating PLC frequency was selected to avoid interference from the lower frequency noise generated by other switching components (e.g. transistors) in the low kHz range. The modem frequency can be adjusted via an external resistor. In this work the one fixed frequency is tested, and data from both boards is divided only in the time domain; it is proposed in future work, frequency and time division multiplexing techniques will be used. In this way, a frequency could be dedicated for urgent messages to permit scalability, where simple polling would add significant delay to step through a large number of modems in a system.

The modem permits digital data signals to be sent and received (i.e. via on-off-keying, OOK) without interpreting the data, enabling flexible data frames and protocols to be developed. Here the modem is linked to a microcontroller, Microchip ATSAMD21E18A, via a RS-232 (UART, Universal asynchronous receiver transmitter) protocol (baud 115.2 kbps).

Higher baud rates or alternative protocols would be possible. In this work for compatibility with the selected microcontroller, UART was

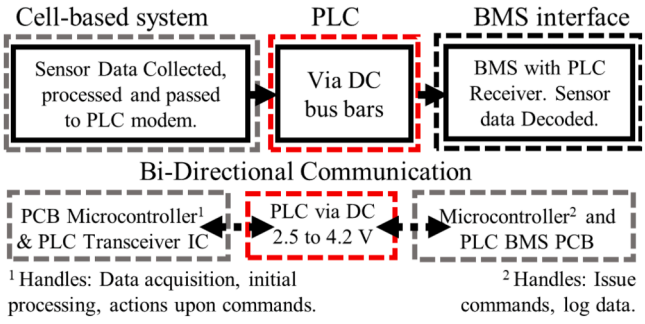

Fig. 1. Block diagram showing components in cell PLC instrumentation system and operation of bi-directional communication.

preferred; other protocols were considered, but would require additional converter integrated circuits (ICs). RS-485 is one alternative, but this may cause the cost and size of the system to be increased due to the required extra ICs.

To form these prototype smart cells, we instrumented 2 × 21,700 cylindrical cells, Fig. 2(a), with thermistor temperature sensors (0201 package size), completed flexible array shown in (b). Each cell was measured to have a static impedance of ~25 mΩ at 25 °C (standard 1 kHz measurement). Due to business confidentially, we are not able to provide the model/manufacturer of the cells, and only the data presented here can be released (raw data files not available). The cells have a capacity of 5 Ah each, thus two in parallel provides a total capacity of 10 Ah. The thermistors were mounted on flexible PCBs to fit inside the dead-space cavity available from the centre mandrel of a cylindrical cell. The cost of each flexible PCB was $0.70, at a low quantity of 200 pieces.

We developed a unique method of instrumenting the cells via a drill forming process, creating a M2.5 hole through the negative terminal, completed assembly shown in Fig. 2(d). This avoids damage to the cell internal components (other methods have involved near complete disassembly [20]), while also minimising the impact on the current collector (internally welded to the aluminium can). Importantly, this type of drilling prevents the generation of swarf or shards of material, which could fall into the cell (risking failure or internal short-circuit). Our process creates a secure fitting point for instrumentation, in a reproducible manner, creating robust sensor insertion; thus, accurate and reliable *in-situ* measurements are possible.

These thermistor sensors were positioned on the flexible PCBs to monitor the temperature at 10 mm spatial resolution along the internal core length of the cell, as shown in Fig. 2(c). Each thermistor array was calibrated prior to instrumentation (20 to 50 °C range) inside a thermal chamber. A 16 bit ADC, Texas Instruments ADS114S08), was used to acquire data from the temperature and current sensors. This was selected offering good resolution (improved compared to built-in 12 bit ADC within microcontroller), small size (QFN32 package), buffered inputs (i.e. compensating for fluctuation in the thermistor resistance) and 12 input channels (9 required here), allowing expansion or a variety of sensors to be used with our platform.

A small (20 mm diameter) PCB, Fig. 3, was designed to incorporate the ADC, microcontroller and PLC modem. The top side was designed to contain the IC components, where the bottom side was dedicated to accessing prototyping connectors (USB, thermistor, expansion etc.). To sense the current through each cell, we designed bus bar current sensors based on an ACS37612 (Allegro Microsystems, USA,) Hall effect IC.

The total assembled cost of each PCB is around $15, which is largely attributed to the costs of the ADC and microcontroller. These costs could

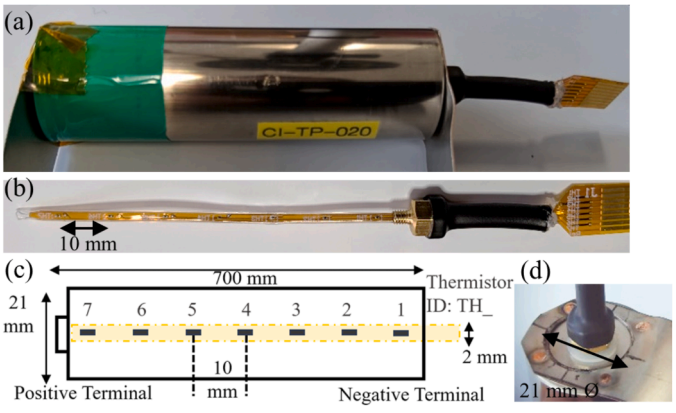

Fig. 2. Assembly of the sensor components for the instrumented cell, (a) overview of instrumented 21,700 cell, (b) thermistor flexible PCB prepared for instrumentation, (c) view of negative terminal of cell post instrumentation, (d) diagram showing layout of thermistor instrumented cell.

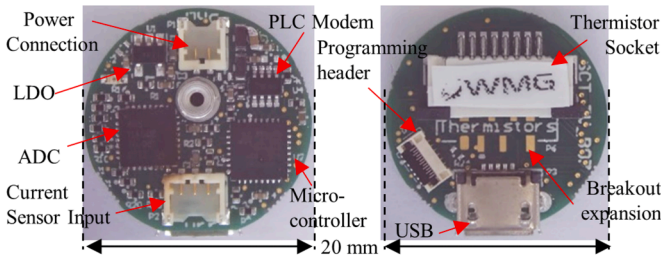

Fig. 3. Photographs of smart cell interface PCB, top side comprises ICs to acquire sensor data and PLC modem, bottom side - prototyping connectors.

significantly be reduced by using 'low-cost' versions of the chips, although for this work, the components for selected to provide a precise and reliable measurement system, with less focus on cost per cell (noting also, a significant reduction in cost would also be realised if ordering in larger quantities, whereas here, component quantities are typically <100 pieces).

The assembled instrumented cells along with the PLC system were placed inside a climate chamber (environment set 25 °C), as shown in the schematic in Fig. 4(a). A photograph of the assembled test setup is shown in Fig. 4(b). A reference performance test (RPT) was designed to verify the instrumentation process was not detrimental to cell performance (in terms of capacity, impedance, energy output capability). This test was performed on a cell cycler (Biologic VSP-300 Potentiostat) using a custom cell holder rig. It involves charging and discharging the cells to the maximum specified limits by the manufacturer at various states of charge; this full discharge and charge cycle enables the capacity to be analysed. The current profile is shown in Fig. 6(a); this profile has also been used in previous work [24]. The current profile first involves a C/2 discharge (5 A) to full charge and then a 1C (10 A) discharge (current values and C rates shown are as considering this 2 parallel cell layout). The RPT profile also includes a series of pulse discharges (1C rate for 30 s). This enables the resistance of the cell to be calculated, which will be evaluated in future work.

It is typical for a microcontroller or ADC IC to require a 3.3 V DC supply for correct operation. In this work, as the circuitry is powered directly from the cells, the voltage can fall below this minimum level (cell voltage 2.5 to 4.2 V). To ensure the monitoring system functions regardless of state of charge, a buck-boost regulator (Maxim Integrated, USA, MAX20344) was trialled in the instrumentation circuit.

During this experiment, data were logged at 10 Hz from each cell via PLC (full 16 bit ADC resolution maintained), with data logged also via a dedicated USB connection for comparison. Each slave data message consists of 25 bytes: Board ID (2 bytes), status indicator (1 byte), 9 channels of sensor data (18 bytes total) and the timestamp (4 bytes). The PLC system enables a flexible addressing system to be developed (here, we can communicate with a specific board via an ID number). In future work, the system could be scaled-up, using this addressing system. The sampling rate of each individual board can be adapted, or perhaps message length reduced (via reducing ADC resolution, for example), to allow a greater number of cells to be connected in series and parallel, while maintaining a thorough level of instrumentation.

In this work, external cell temperature data were measured via a thermistor array mounted on the surface of the can (orientation aligned with internal array) as well as an external thermocouple (TC-08, Pico Technology, UK), located centrally. Custom software for the data logging PC was developed to monitor cell data in real-time.

4. Results and discussion

Data were logged continuously via PLC for the ~24 hr experiment, with identical data successfully logged via both the dedicated wired USB connection and PLC (approximately 400,000 data messages were transmitted from each cell interface board). No missing communications

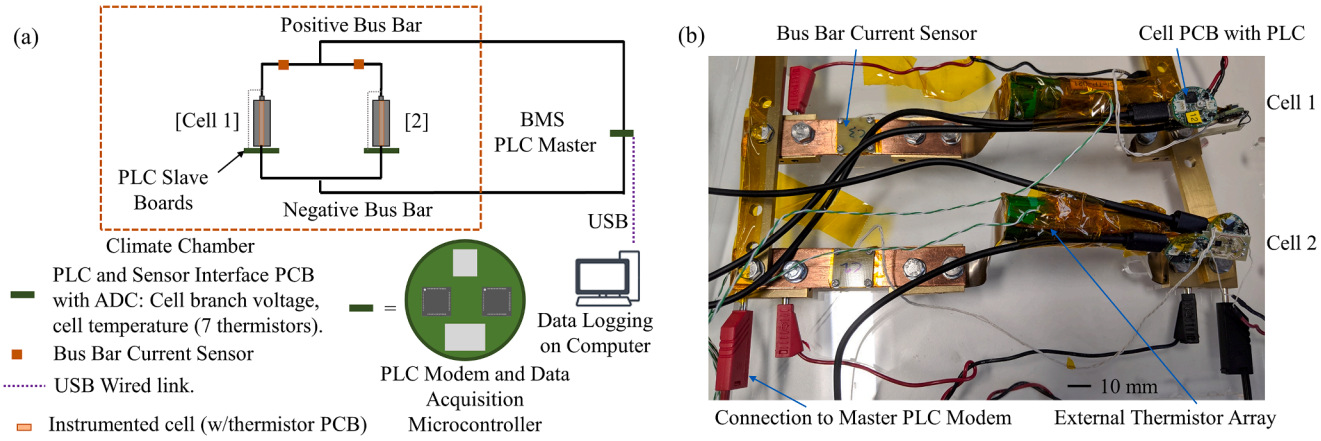

Fig. 4. (a) Schematic of the 2P cell configuration, showing the climate chamber, instrumented cells and interface/PLC PCBs, (b) Photograph of the assembled 2-parallel instrumented cell rig – Internal and External thermistor arrays are inserted-into and attached-onto each cell, respectively.

were reported (the master is configured to output an error message if a response from a slave board is not received within an allocated time of 20 ms). This was confirmed by comparing the data received by USB and PLC; Fig. 5(b) shows no differences in the data were detected. To analyse if there was any significant delay between the data being received by the PLC modem and if the data was collected via a dedicated USB connection, timestamps were also logged on the receiving computer. The delta time between USB and PLC received data, Fig. 5(a), demonstrates the processing required to handle receiving data outweighs the transmission time over the power line (~20% of messages recorded as being received via the PLC modem before the dedicated USB connection). A future study with improved real-time message handling is required to determine the precise time penalty, if any, for transmitting via PLC.

To verify the PLC system was capable of operation across the full state of charge range (not shown in our previous studies [5]), the cell was discharged and charged as shown in Fig. 6. The profile (a) shows the cells were tested across high charge and discharge rates (up to 1C, 5 A discharge per cell, negative values indicate discharging). The voltage readings (b) indicate the full state of charge (0%, 2.5 V to 100%, 4.2 V) was explored.

The data in Fig. 6(a) demonstrates the success of our bus bar mounted current sensor, where the current applied to each cell can be accurately tracked (cells arranged in 2P, thus individual current ~ half current value applied from cycler). The majority of the data in these experiments to verify the PLC operation was gathered from the flexible thermistor arrays (7 sensors, 16 bit ADC data transmitted). The data, cell

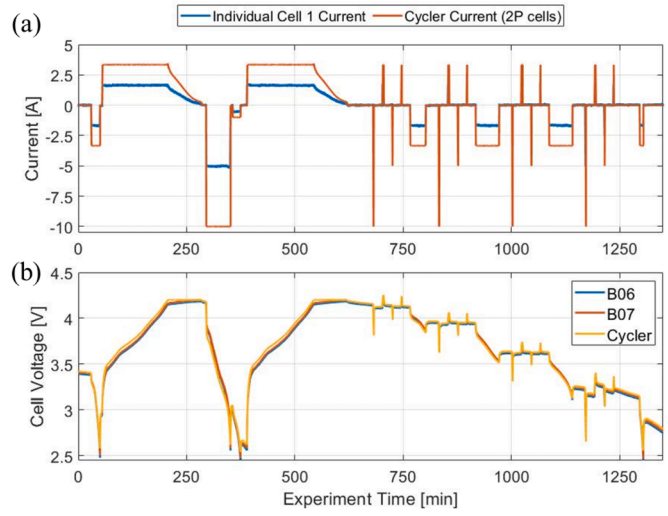

Fig. 6. (a) Current profile applied by cycler and individual current measured via Hall effect bus bar sensor, (b) voltage recorded via cycler and for each cell across experimental period.

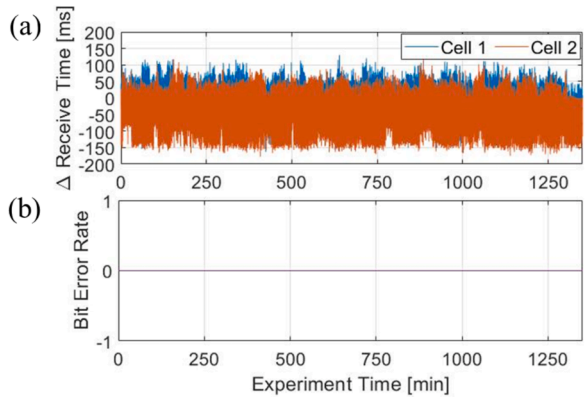

Fig. 5. (a) Time offset between messages received on data logging computer via USB and PLC (positive values indicate PLC received first), (b) Errors detected between data received via USB and PLC for all 18 sensors (current, voltage and temperature), comparing ADC 16 bit values.

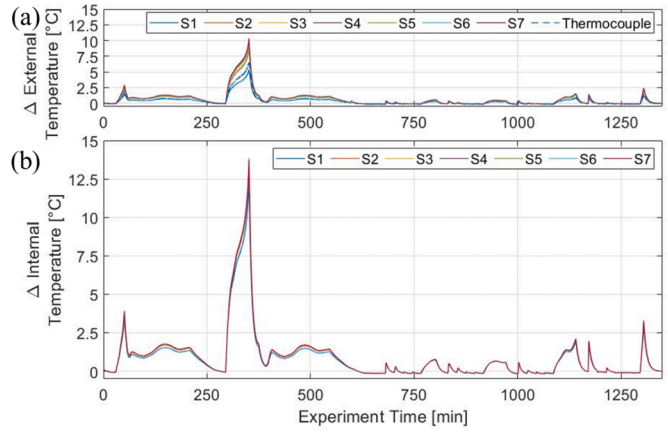

Fig. 7. Thermistor and reference thermocouple data (Cell 1), (a) externally (surface can) cell measurements acquired via dedicated USB connection, (b) internal thermistor (core) temperature data acquired via PLC.

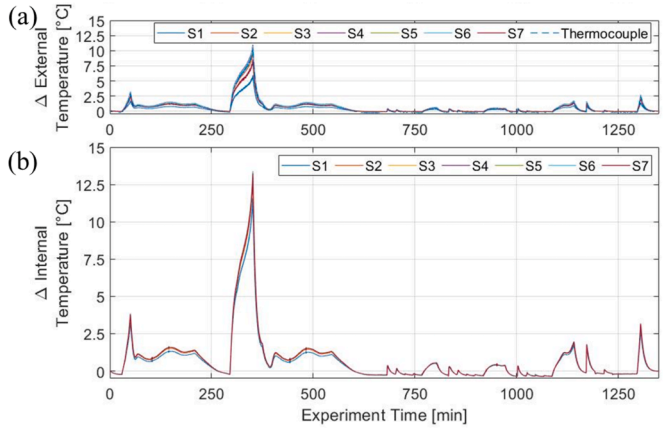

Fig. 8. Cell 2 temperature data recorded, (a) external (surface can) cell measurements acquired via dedicated USB connection, thermistor and thermocouple (placed centrally near S4) measurements, (b) internal thermistor (core) thermistor temperature data acquired via PLC.

1 internal and external data in Fig. 7(a) and (b), and cell 2 internal and external data in Fig. 8(a) and (b), respectively, demonstrate the successful transfer of data via PLC. In the case of both cells, a notable temperature difference between surface and core temperature is apparent (peak after prolonged 5 A discharge, core temperature is ~3.4 °C hotter, positive terminal noted as hottest location).

This temperature difference corresponds to existing data in the literature, although uniquely here a low-cost thermistor array is implemented (fibre optic sensors have previously been studied to provide distributed cell core data) [11]. The positioning of the external thermocouple on cell 1, Fig. 7(a), is shown to exhibit a lower peak temperature increase (~2.5 °C lower than cell 2). In previous work, without PLC, we noted a cell can temperature increase of ~10 °C is expected when this RPT profile is cycled.

In this experiment we have demonstrated 18 sensors (7 temperature, 1 Vage, 1 current, per cell) can be transmitted with 100% success rate via PLC (10 Hz data sampling rate). As we discussed previously (4S2P setup, [5]), the PLC network we have developed is designed to be flexible in terms of number of nodes (cells) in the network and sensors (quantity and type) installed. In this example, the 18 sensors were distributed across 2 cells, however, if a particular application required only 1 sensor per cell, 18 cells could be instrumented without further demand on the PLC network bandwidth. This work did not aim to load the network to maximum capacity; future work could involve testing with additional sensors and faster sampling rate (perhaps thereby requiring faster baud rate) to determine the practical capacity of the system.

Detailed measurements as demonstrated in this work, provide valuable data for pack design, and understanding cooling system operation and cell temperature gradients. Considering this same PLC bandwidth (18 sensors, 10 Hz rate) using a single channel/frequency, the system could be expanded to various configurations, increasing the number of cells (nodes) in the network, while reducing the number of sensors per cell – examples are shown in Table 1. In the application of instrumenting a pack, a tens or hundreds of cells may be acquiring data. In the case where thorough instrumentation was required (i.e. multiple sensors per cell), adaptive sampling rates would be beneficial. Fig. 9 demonstrates how by reducing the sampling rate to < 1 Hz during normal operation, the single PLC channel can remain 'available' (not in-use) to receive critical or alert messages. Critical messages might be required when the cell is operating outside the safe regions, while alert may be when it is operating close to these limits. Sampling at a lower rate would mean important data points would be missed, therefore variable sampling rates are required to balance periods of inactivity with periods of interest.

In future work we will demonstrate an adaptive sampling system, using bi-directional communication. In Scenario 4 below, the cell PCB transmits an alert message to the master when higher sampling rates are required. As the system generally only polls at 0.5 Hz during normal operation, there is adequate 'available' time periods between polling each cell to receive these alert messages. Thus, the system is able to respond to requests to acquire critical data within a maximum period of 50 ms, as the alerts can be triggered at any time when the system is not using the channel (i.e. acquiring data from polling a cell). This assumes the system will only need to acquire data at a critical rate up to a maximum of 2 cells from the 4 cell system. Further details of this adaptive sampling scheme will be described in an upcoming dedicated article on the smart PLC system.

The buck-boost regulator enabled a constant 3.3 V DC supply was available to power the PLC IC and associated circuitry (total estimated power consumption ~ 110 mW during transmission). The lowest voltage (~2.5 V recorded at ~375 and 1300 min time periods) did not affect the operation of the communication network (the power line voltage itself is the voltage recorded by the cycler and cells, where the regulated voltage is required only for the ICs). The low voltage sections were not maintained for period < 30 min, else the cells would become discharged below their normal operating region (i.e. due to system requiring power from cell). The operating power requirements were greater in this experiment compared to a real-world scenario, where data were sampled (10 Hz) faster than required for cells during rest (perhaps 1 Hz or slower is sufficient, if no significant change in voltage, current or temperature detected).

Table 1
Example scenarios (Sn) to divide bandwidth as used in this work between a different number of cells in a network.

Sn#	#Cells	Notes
#1	2	Current work. 9 sensor data values sent at 10 Hz per cell.
#2	18	Only 1 sensor data value per cell, allows up to 18 cells, 10 Hz.
#3	18	9 sensor data values per cell, reduces sampling to 0.5 Hz.
#4	4	9 data values per cell, with adaptive sampling. E.g. 0.5 Hz low, 5 Hz Alert Operation, 10 Hz critical (assuming max. 2 cells simultaneously).

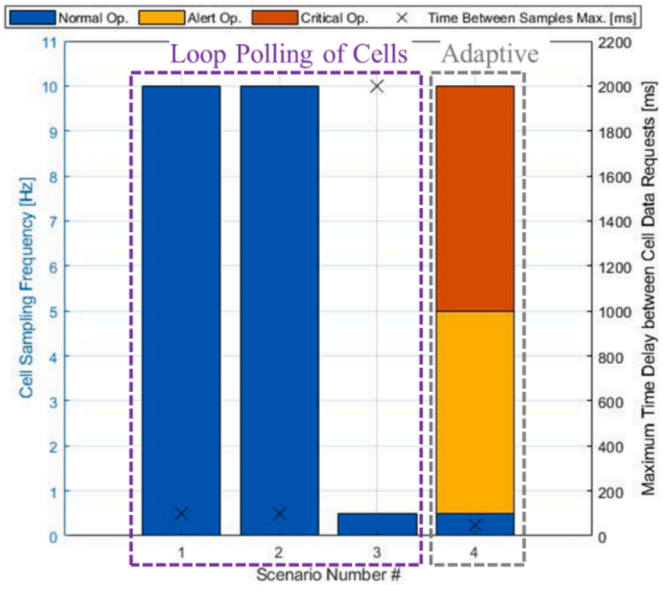

Fig. 9. Visual representation of the sampling schemes. Scenario #4 highlights possible future work with adaptive sampling.

5. Conclusions

In this work we have successfully demonstrated our unique PLC network offers the opportunity to instrument cells (temperature, current and voltage sensors) without the burden of heavy, bulky, and perhaps fragile communication cabling. The system functioned (0 errors detected compared to dedicated wired connection and minimal delay) across the full state of charge range of the 21,700 cells (2.5 to 4.2 V tested).

The importance of understanding cell core temperature was noted, where external temperature lags core measurements, and core temperatures are considerably hotter (>3 °C delta recorded). The PLC system is adaptable to accommodate sensors needed to gather comprehensive data to aid modelling and pack development work. Here, three types of sensor (voltage ADC, thermistor, Hall effect) were shown.

PLC provides a reliable bi-directional communication link, and in our testing using a data logging computer, messages were received within 150 ms region (compared to a dedicated wired connection), and in some instances (~20% occurrence) data were received in advance, thereby indicating the indiscernible time delta limitation of our current data logging configuration.

6. Further work

6.1. PLC System development

The PLC modem (TI THVD8000DDFR) was not utilised to full capacity during this work, where the lower baud rate (115.2 kbps compared to possible 500 kbps) restricted the data transfer rate, and therefore system bandwidth. This could be investigated in future work, to assess maximum system capability. Furthermore, only 18 sensors were used in this work. We proposed additional sensors could be added (or distributed broadly across a greater number of cells) to enable module or pack testing. The possibility of an adaptive sampling scheme was discussed, to reduce the bandwidth usage of the PLC channel when the cells are in a low or normal operating condition. This would help expand the system to include a larger number of sensors (and/or cells), while permitting interrupts to quickly be sent from a given cell, to alert the master it is experiencing an abnormal event. We will discuss this topic further, and provide data driven examples in an upcoming article.

This work demonstrated operation between the full voltage range of the cell, although this could further be expanded to understand operation at a module level. This could include validation of PLC over a commercial bus bar design that comprises multiple materials and welds. In later work, we will publish a comparison against an alternative network topology (CAN), although SPI (Serial Peripheral Interface) or LIN (Local Interconnect Network) could also be tested. In future work, we also plan on testing a greater number of cells (in a different series and parallel arrangement) to verify the system can be scaled, and to verify PLC functionality in a larger network.

To account for potential noise sources during a real-world application, it is proposed further data integrity checks would be needed to maintain the 100% transmission success currently achievable. The time penalty involved with PLC transmission compared to other topologies (i.e. at least a dedicated wired connection) must be investigated further.

6.2. Instrumented cells

The work could be expanded to create a single IC or single board design (thermistor array and interface electronics together). The array itself could be varied (thermistor location, density) to investigate the heating at a specific region of the cell. The PLC network constructed in this work was designed to capture data from a variety of sensors (analogue and digital, e.g. SPI or I2C could be added). In the future we propose expanding our sensing capabilities, involving multi-sensor type arrays, based on the instrumentation process developed in this work.

Acknowledgements

This work was funded by EPSRC, Jaguar Land Rover Limited and WMG University of Warwick, under the Prosperity Partnership grant, R004927.

References

[1] Y. Huang, C. Li, Real-time monitoring system for paddy environmental information based on DC powerline communication technology, Comput. Electron. Agric. 134 (Mar. 2017) 51–62, https://doi.org/10.1016/j.compag.2017.01.002.
[2] S.-.D. Ma, M.-.S. Park, J.-.E. Kim, DC-PLC Modem design for PV module monitoring, J. Int. Counc. Electr. Eng. 6 (1) (Jan. 2016) 171–181, https://doi.org/10.1080/22348972.2016.1217817.
[3] M. Brandl, K. Kellner, T. Posnicek, D. Hochwarter, Performance evaluation of a DQPSK and a DSSS PLC-modem for vehicular applications, in: Proceedings of the 2019 IEEE International Symposium on Power Line Communications and its Applications, ISPLC, 2019, pp. 1–5, https://doi.org/10.1109/ISPLC.2019.8693264, 2019.
[4] W.-.W. Hu, F.-.L. Chang, Y.-.H. Zhang, L.-.B. Chen, C.-.T. Yu, W.-.J. Chang, Design and Implementation of a Next-Generation Hybrid Internet of Vehicles Communication System for Driving Safety, JCM 13 (12) (2018) 737–742, https://doi.org/10.12720/jcm.13.12.737-742.
[5] T.A. Vincent, J. Marco, Development of smart battery cell monitoring system and characterization on a small-module through in-vehicle power line communication, IEEE Access (2020), https://doi.org/10.1109/ACCESS.2020.3043657.
[6] Y.H. Zhang, et al., An implementation of an in-vehicle power line communication system, in: 2017 IEEE 6th Global Conference on Consumer Electronics, GCCE 2017, 2017, pp. 1–2, https://doi.org/10.1109/GCCE.2017.8229422, vol. 2017-Janua.
[7] M.S. Saleem, Development of PLC based communication architecture for battery management system, in: IEEE Vehicular Technology Conference 2020, 2020 vol., doi: 10.1109/VTC2020-Spring48590.2020.9128451.
[8] T.F. Landinger, G. Schwarzberger, G. Hofer, M. Rose, A. Jossen, Power line communications for automotive high voltage battery systems: channel modeling and coexistence study with battery monitoring, Energies 14 (7) (Mar. 2021) 1851, https://doi.org/10.3390/en14071851.
[9] A.P. Talie, W.A. Pribyl, G. Hofer, Electric vehicle battery management system using power line communication technique, in: PRIME 2018 - 14th Conference on Ph.D. Research in Microelectronics and Electronics, 2018, pp. 225–228, https://doi.org/10.1109/PRIME.2018.8430304.
[10] J. Jousse, N. Ginot, C. Batard, E. Lemaire, Power line communication management of battery energy storage in a small-scale autonomous photovoltaic system, IEEE Trans. Smart Grid 8 (5) (Sep. 2017) 2129–2137, https://doi.org/10.1109/TSG.2016.2517129.
[11] S. Novais, et al., Internal and external temperature monitoring of a Li-ion battery with fiber bragg grating sensors, Sensors 16 (9) (Aug. 2016) 1394, https://doi.org/10.3390/s16091394.
[12] X. Lin, H.E. Perez, J.B. Siegel, A.G. Stefanopoulou, Robust estimation of battery system temperature distribution under sparse sensing and uncertainty, IEEE Trans. Control Syst. Technol. (Jan. 2019) 1–13, https://doi.org/10.1109/tcst.2019.2892019.
[13] R.R. Richardson, S. Zhao, D.A. Howey, On-board monitoring of 2-D spatially-resolved temperatures in cylindrical lithium-ion batteries: part II. State estimation via impedance-based temperature sensing, J. Power Sources 327 (Sep. 2016) 726–735, https://doi.org/10.1016/j.jpowsour.2016.06.104.
[14] S. Baksa, W. Yourey, Consumer-based evaluation of commercially available protected 18650 cells, Batteries 4 (3) (Sep. 2018), https://doi.org/10.3390/batteries4030045.
[15] A. Misra, Energy storage for electrified aircraft: the need for better batteries, fuel cells, and supercapacitors, IEEE Electrif. Mag. 6 (3) (Sep. 2018) 54–61, https://doi.org/10.1109/MELE.2018.2849922.
[16] T. Faika, T. Kim, M. Khan, An internet of things (iot)-based network for dispersed and decentralized wireless battery management systems, in: 2018 IEEE Transportation and Electrification Conference and Expo, ITEC, 2018, pp. 342–346, https://doi.org/10.1109/ITEC.2018.8450161, 2018.
[17] G.M. Cavalheiro, T. Iriyama, G.J. Nelson, S. Huang, G. Zhang, Effects of nonuniform temperature distribution on degradation of lithium-ion batteries, J. Electrochem. Energy Convers. Storage 17 (2) (May 2020), https://doi.org/10.1115/1.4045205.
[18] P.V. Chombo, Y. Laoonual, A review of safety strategies of a Li-ion battery, J. Power Sources 478 (Dec. 2020), 228649, https://doi.org/10.1016/j.jpowsour.2020.228649.
[19] T. Grandjean, A. Barai, E. Hosseinzadeh, Y. Guo, A. McGordon, J. Marco, Large format lithium ion pouch cell full thermal characterisation for improved electric vehicle thermal management, J. Power Sources 359 (2017) 215–225, https://doi.org/10.1016/j.jpowsour.2017.05.016.
[20] J. Fleming, T. Amietszajew, J. Charmet, A.J. Roberts, D. Greenwood, R. Bhagat, The design and impact of in-situ and operando thermal sensing for smart energy storage, J. Energy Storage 22 (October 2018) 36–43, https://doi.org/10.1016/j.est.2019.01.026, 2019.
[21] Z. Wei, J. Zhao, H. He, G. Ding, H. Cui, L. Liu, Future smart battery and management: advanced sensing from external to embedded multi-dimensional measurement, J Power Sources 489 (2021). Elsevier B.V., p. 229462, 31-Mar.

[22] C. Alippi, C. Alippi, Intelligent mechanisms in embedded systems. Intelligence For Embedded Systems, Springer International Publishing, Zurich, 2014, pp. 159–210.
[23] Texas Instruments, Online Datasheets, 2021. https://www.ti.com/product/THVD8000 [Online]. Available: https://www.ti.com/product/THVD8000.
[24] Y. Yu, et al., Distributed thermal monitoring of lithium ion batteries with optical fibre sensors, J. Energy Storage 39 (Jul. 2021), 102560, https://doi.org/10.1016/j.est.2021.102560.